Rate effect on lithium-ion graphite electrode performance

T. D. TRAN, J. H. FEIKERT, R. W. PEKALA

Chemistry & Materials Science Department, Lawrence Livermore National Laboratory, Livermore, CA 94550, USA

K. KINOSHITA

Energy and Environment Division, Lawrence Berkeley National Laboratory, Berkeley, CA 94720, USA

The electrochemical performance of lithium-ion graphite electrodes with particle diameter in the range of 6–44 μm was evaluated at different discharge (intercalation)/charge (deintercalation) rates (C to $C/60$). The electrode capacity depends on both the average particle size and rate. With a simple rate programme, the electrode performance is dependent on the cycling rate. The capacity of small graphite particles (6 μm) at $C/2$ rate was 80% of that achieved at $C/24$ rate ($\sim$372 mAh g^{-1}). The capacity of large graphite particles (44 μm) obtained at fast rates ($C/2$) was only 25% of that obtained under near-equilibrium conditions ($C/24$). The electrode capacity, however, is nearly independent of the charge rate when the electrode is fully intercalated using a modified rate programme containing a constant-voltage hold at 0.005 V (vs Li$^+$/Li) for several hours. The electrochemical behaviour is related to the physicochemical properties of the graphite particles.

1. Introduction

Electrochemical lithium intercalation/deintercalation in nonaqueous electrolytes occurs reversibly in many carbonaceous materials. Under near-equilibrium conditions (i.e., at low rates of intercalation/deintercalation), the lithium storage capacities of various conventional carbons (exposed to $T > 1000\,^\circ$C) and graphites approach 372 mAh g^{-1}, corresponding to one mole of lithium for every six moles of carbon (LiC$_6$). This lithium capacity, however, is a function of the discharge (intercalation)/charge (deintercalation) rate and tends to be lower at higher rates. To obtain the maximum capacity of the carbon materials, lithium intercalation/deintercalation experiments are generally carried out at slow rates to facilitate both kinetic and transport processes. Aurbach and Ein-Eli [1] investigated Lonza KS44 synthetic graphite at different current densities and found that the $C/7$ rate is the highest rate possible for these electrodes (0.1–0.2 mm thick, 44 μm particle diameter) in which full capacity (*ca.* Li$_{0.92}$C$_6$) was obtained. The $C/7$ rate is equivalent to a constant current discharge or charge of a carbon electrode to its full capacity (assumed to be LiC$_6$) in 7 h. Rates as slow as $C/600$ were used by Dahn and coworkers [2] to avoid kinetic complications and to ensure reversible conditions for determining thermodynamic parameters. In experiments with a large number of carbonaceous materials with a wide spectrum of physical and structural properties, we [3] have found that the $C/24$ rate is sufficiently slow to attain the maximum lithium capacity for insertion/deinsertion processes. The maximum

capacity obtained under these conditions, as well as the characteristic plateaus associated with staged phases, are reproducible in successive cycles in many graphite materials. In our work with half-cell studies employing a lithium counter electrode, the discharge of a carbon electrode represents the intercalation of lithium into the electrode. The charging process involves lithium deintercalation.

Experimental measurements that consist of constant-current discharge and charge steps between predetermined cutoff voltages are useful for obtaining information on the effect of rate on the lithium capacity. Carbon electrodes exhibit different current–voltage profiles that are characteristic of the intercalation/deintercalation process. The discharge/charge characteristics at different current densities of several carbons were investigated by Zhang [4] using cyclic voltammetry and galvanostatic techniques. The intercalation process was found to be the slow step in the carbon cycling experiments. Empirical charging (intercalation) kinetics parameters tend to decrease with increasing crystallinity of the carbon materials [4]. The electrode capacities were nearly independent of (deintercalation) current densities when they were fully charged. Recently, Takami and coworkers [5] reported that the rate capability of graphitized carbon fibres was superior to that of graphite particles. The decrease in the capacity of the graphitized carbon fibre was significantly smaller than that of graphite with increasing current density. When the current density increased from 0.25 mA cm^{-2} ($C/$15 rate) to 5 mA cm^{-2} (1.3 C), the carbon fibre capacity decreased by only 10% whereas the graphite capacity dropped by 50%. The radial-like texture of

the fibre contributed to rapid lithium diffusion, resulting in its high rate capability. Typical dimensions of these fibres are 8 μm diameter and 60 μm length.

The performance of carbon electrodes also depends on the particle size [6, 7]. Tarascon and Guyomard [6] observed that the reversibility of electrochemical Li intercalation is strongly dependent on the particle size of graphite, when the results are obtained at the same current rate. In particular, better performance and less irreversibility were obtained with very fine graphite particles ($<1\,\mu$m diam.). Peled *et al.* [7] also observed that the reversible intercalation of Li into graphite was dependent on the particle size. Detailed results, however, were not available. Zaghib and coworkers [8] investigated the electrochemical behaviour of graphite whiskers of various dimensions. The capacity was found to depend strongly on both fibre diameter and length. The optimum performance was obtained from chopped graphitized fibres that were 2 μm diameter and 23 μm length, yielding 363 mAh g^{-1} reversible capacity and an irreversible capacity loss as low as 20 mAh g^{-1}.

Carbon electrodes with the capability for high-rate intercalation/deintercalation of lithium are of practical interest for lithium-ion batteries for electric vehicle applications. This study was prompted by the requirement of high-power density for lithium-ion batteries used in electric vehicles. In this work, we investigated the effect of rate on the performance (capacity, capacity loss) of electrodes containing synthetic graphite particles of varying average diameters. Factors which influence the capability of graphite electrodes at high currents are elucidated, and the results are correlated with their physical and chemical properties.

2. Experimental details

Electrochemical studies were performed using a 64-channel Maccor battery tester. The experiments were carried out in a 15 ml, three-electrode cylindrical cell in which the electrodes and separator were positioned horizontally and stacked vertically. The geometric surface area of the working electrode was 1.12 cm^2 and its thickness was 0.3 mm. The electrodes containing the graphite powders were prepared according to a procedure described earlier [3]. They weighed approximately 19 mg and contained about 80% graphite powder, 12% phenolic-resin derived carbon binder and 6% carbon paper. Lithium foils (Cyprus Foote Mineral) were used as the counter and reference electrodes. Whatman fibreglass filters (934-AH) was used as the separator between the working and counter electrodes. The electrolyte was 0.5 M lithium trifluoromethanesulfonimide, LiN-(CF$_3$SO$_2$)$_2$, (tradename HQ115, 3M Corp) in a 50:50 mixture of ethylene carbonate and dimethyl carbonate (Grant Chemical). The cells were constructed and tested at 20 $\pm$ 2 °C in a dry argon-atmosphere glove box ($<$ 10 ppm water).

The experiments were performed with Lonza G+T Ltd (Switzerland) synthetic graphites having average particle sizes ranging from 6–44 μm. According to the manufacturers specification sheets, these graphite materials have narrow particle size distributions with the average particle diameter denoted by the trade-name suffix (e.g., SFG6 has average particle size of 6 μm). These graphites are highly anisotropic synthetic graphites which were heat treated at temperatures up to 3000 °C before grinding and then fractionated to the appropriate particle size range. TEM and SEM observations show that these graphite particles resemble flat platelets (flat lamellae) with well-defined basal planes. The physical and structural characteristics of Lonza graphites are tabulated in Table 1.

Two cycling procedures were used: (i) the simple rate programme, that is, the rate of discharge (intercalation) / charge (deintercalation) is symmetric in that each half-cycle consists of a constant-current step at rates between C to $C/60$ to a cutoff voltage of 0.005 V (Li$^+$/Li) during discharge and at 1.5 V during charge; and (ii) the modified rate programme, that is, the half-cycles are the same as (i) but with additional constant-potential holds for several hours at 0.005 V and 1.5 V after reaching these voltage limits. The second procedure allows sufficient time to minimize concentration polarization effects and to ensure more complete lithium intercalation or deintercalation.

3. Results and discussion

The electrochemical performance of Lonza graphites at a slow rate ($C/24$) have been examined earlier [3]. The results are in good agreement with those reported by others [5, 9] who also examined these materials at relatively low current densities (equivalent to $C/15$–$C/600$ rates). The graphite potential profiles are flat and contain at least three plateaus characteristic of staged phases in region below 250 mV (vs Li$^+$/Li). The reversible capacities observed with these materials are about 330–360 mAh g^{-1}, (corresponding x values of 0.90–0.96 in Li$_x$C$_6$ composition). Their performance and related physicochemical properties are listed in Table 1.

3.1. *Effect of the simple rate programme on graphite particle performance*

The discharge/charge profiles of SFG6–SFG44 at constant-current rates, $C/2$, $C/8$ and $C/24$, are shown in Fig. 1(a)–(c), respectively. Polarization effects are clearly evident at high rates (Fig. 1(a)). The high overpotentials dominated the potential response, and the electrode potential reached the lower cutoff limit (0.005 V) in significantly less time than that projected. For example, at the $C/2$ rate, the SFG6 electrode potential reached the lower limit of 5 mV in 90 min instead of 120 min in the first cycle. Consequently, the first cycle reversible capacity of SFG6 graphite at the $C/2$ rate decreased to 75% of that obtained at the $C/24$ rate. In successive cycles, the polarization

Table 1. Physicochemical properties* and performance data[†] of Lonza synthetic graphites

Sample	Particle size /μm	BET area /$m^2 g^{-1}$	L_c /nm	d_{002} /nm	x in Li_xC_6	Irr. cap. loss /mAh g^{-1}
SFG6	6	15.2	> 100	0.336	0.95	70
SFG15	15	8.8	> 120	0.336	0.90	64
SFG44	44	4.2	< 200	0.336	0.93	108

* Data obtained from manufacturer information sheets.
[†] Electrolyte is 0.5 M HQ115 / 50:50 EC:DMC. C/24 rate.

continues to influence the potential response. In the fourth cycle, the lower limit was reached in only 25 min so lithium intercalation was terminated prematurely. The effects of the rate are more pronounced on the larger particles as evident by the rapid decrease in potential with lithium intercalation shown in Fig. 1(a) and (b). The characteristic (i.e., equilibrium) constant-potential plateaus associated with lithium staging in the graphite structure are apparent at the C/24 rate (Fig. 1(c)) or at a slower rate. Three apparent plateaus can be observed from the profiles for various particle sizes obtained at the C/24 rate. In successive cycles, electrode behaviour remains reproducible, indicating negligible effects from mass transport and reversible intercalation/deintercalation processes under these conditions.

The effect of rate (as defined in procedure (i)) on the capacity of various particles is shown in Fig. 2. The electrode capacities depend on both the rate and cycle number. The (deintercalation, first cycle) capacity for SFG6 at C/2 rate was 295 mAh g^{-1} ($x = 0.79$). It continued to drop with cycle number and decreased by as much as 80% after the tenth cycle, as in Fig. 2. Incomplete discharge as the result of concentration and charging overpotentials appears to have a cumulative effect. Since the intercalation process is slower than the deintercalation process [4, 10], continued cycling at a high rate results in the reduced utilization of certain storage sites in the graphite structure, even for particles as small as 6 μm diameter. The rate effect on capacities of larger particles is more pronounced. The x values for SFG15 and SFG44 decreased much more rapidly than that of SFG6 at higher rates and increasing cycle numbers. The reduced capacities at fast rates do not, however, affect the intrinsic (maximum) capacities of the graphites. The initial high capacities were recovered when the electrodes were cycled at the slow C/24 rate.

The effect of the average particle size and intercalation/deintercalation rate on the Li intercalation capacity is summarized in Fig. 3. It is apparent that the capacity of the graphite with large particles is very sensitive to the rate. Both Lonza SFG15 and SFG44 (average particle size 15 μm and 44 μm, respectively) exhibit low capacity ($x \sim 0.2$) at the C/2 rate. On the other hand, the small particles (Lonza SFG6) were able to maintain a capacity of $x \sim 0.8$ at this rate. Only when the rate was lowered to C/24 does the large particles show capacities of x above 0.9.

3.2. Qualitative analysis of transport and ohmic processes

The decrease in capacity of graphite at high discharge/charge rates can be attributed to overpotentials associated with three transport processes that are involved in the intercalation process. These are (i) transport of lithium ions in the electrolyte to the surface of the graphite electrode (ii) diffusion of lithium ions through the solid–electrolyte interphase (SEI) and (iii) lithium diffusion in the bulk graphite structure. The relative importance of these three transport processes can be evaluated qualitatively by examining the relative diffusion times in the various phases. To a first approximation, the characteristic diffusion time is defined as L^2/D [11], where L is the diffusion length and D is the diffusion coefficient. The diffusion time in the three phases (liquid, SEI and graphite) were compared for different particle sizes, and the results are summarized in Table 2. D is assumed to be constant in these calculations for simplicity.

For transport in the liquid phase, the diffuse layer thickness is assumed to be 10^{-3} cm. The data for the diffusion coefficient of lithium ions in an EC/DMC-based solvent is not available. However, a typical value in a carbonate system is on the order of 10^{-5} cm^2 s^{-1} [12]. Under these conditions, a representative diffusion time for the lithium ion in the electrolyte phase is < 0.002 min.

The transport of lithium in the SEI layer has not been studied extensively, but it is generally regarded as fast, considering the microcrystalline nature of this passivating layer [13]. Lithium was thought to diffuse primarily in the grain boundaries. The diffusion coefficient of lithium in the SEI film was reported to be 2×10^{-5} cm^2 s^{-1} [8, 12]. Taking into consideration the relatively thin ($\sim$ 5–50 nm, [13]) diffusion length (i.e., solid-electrolyte interphase), lithium transport in the SEI should not be the rate-limiting factor.

The effective length for lithium diffusion in the Lonza graphite is assumed to be the particle radius. The diffusion coefficient of lithium in artificial graphite was found by Takami and coworkers [14] to decrease almost linearly with capacity up to $x = 0.5$ and tended to level out at around 10^{-9} cm^2 s^{-1} with $0.5 < x < 1.0$. Sato et al. [15] reported a similar dependence of the diffusion coefficient on x values during both lithium intercalation and deintercalation. Hysteresis was not observed. For the purpose of this analysis, an average diffusivity of 10^{-9} cm^2 s^{-1} was
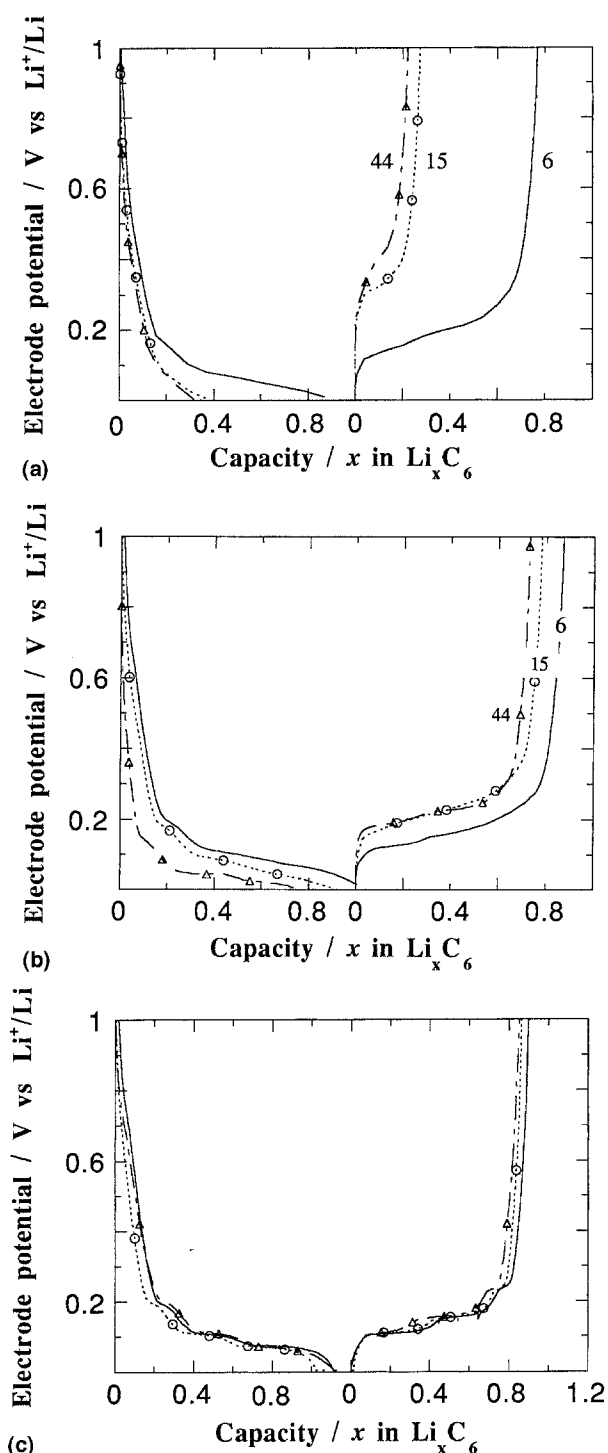
Fig. 1. Potential profiles (first cycle) of Lonza SFG6-SFG44 graphites in 0.5 M LiN(CF₃SO₂)₂ / 50:50 EC–DMC at (a) $C/2$ rate, (b) $C/8$ rate and (c) $C/24$ rate. Number on graph indicates average particle size. Discharge/charge programme involves constant current rates between 0.005 V and 1.5 V limits. Key (c): (——) 6 μm; (O · · · · O) 15 μm; (△——△) 44 μm.

used. The time required for sufficient transport of lithium ions into the graphite particles varies from 1.5 min to 78 min for particles ranging in diameter from 6 to 44 μm. Under these conditions, a constant rate for 2 h ($C/2$) should be sufficient to achieve complete lithium intercalation.

The effect of ohmic (IR) polarization on the capacities at fast rates was analysed. The internal resistance of the cells used in this study was determined by the current-interruption method to be approximately
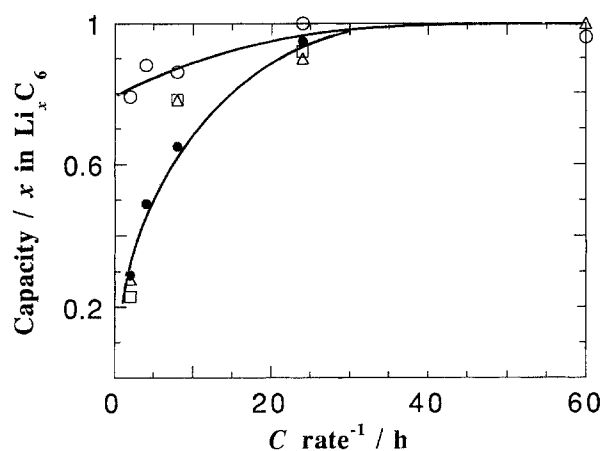

Fig. 2. Reversible capacities (x in Li$_x$C₆) as a function of charge/discharge rate for various particle sizes: (O) 6 μm, 1st cycle; (●) 6 μm, 10th cycle; (△) 15 μm, 1st cycle; (□) 44 μm, 1st cycle.

60 Ω. This is equivalent to an overpotential of 16 mV at the $C/24$ rate and 380 mV at the C rate. The ohmic overpotential is reflected in the initial potential drop prior to the onset of deintercalation (see Fig. 1(a)–(c)). Even at a very slow rate ($C/100$), Shu *et al.* [10] have shown that ohmic resistance can affect the lithium deintercalation capacities of graphite particles of 15 μm average diameter in electrodes with thickness in the range between 0.2–0.65 mm. The IR drop is expected to decrease with larger electrode areas and thinner electrode separation as well as improved electrolyte conductivity.

The ionic resistance of the electrolyte phase in the pores of the electrode can also contribute to the electrode overpotential. This value is estimated by the analytical solution of Risch and Newman [16] for porous packed-bed electrodes. Under the conditions of negligible electrical resistance in the solid carbon structure, the potential difference between the front and the back of the electrode ($\Delta\Phi$) is simplified to the expression $\Delta\Phi = id/2k$ where i is the current density, d is the electrode thickness and k is the (pore) electrolyte conductivity. With a typical k value of $6 \times 10^{-3}\,\mathrm{S\,cm^{-1}}$ [17] and current density of $6\,\mathrm{mA\,cm^{-2}}$ (C rate), the voltage drop across the electrode thickness of less than 0.1 mm is calculated
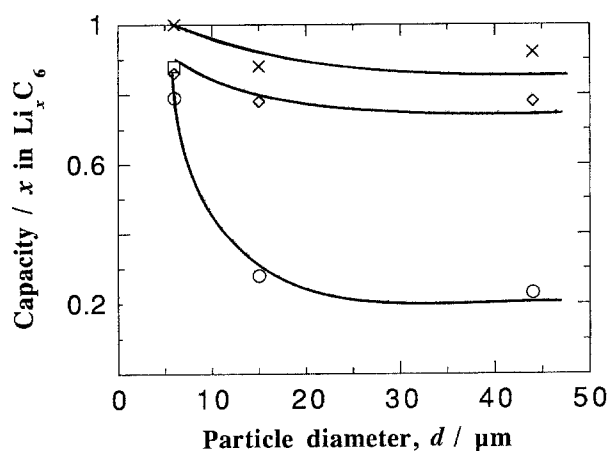

Fig. 3. Capacity as a function of particle diameter at various rates. Electrodes cycled according to the simple rate programme (procedure (i), Section 2). Key (O) $C/2$; (□) $C/4$; (◇) $C/8$; (×) $C/24$.

Table 2. Characteristic diffusion time for various electrode transport processes

Particle size /μm	Characteristic diffusion time, L^2/D /h		
	Electrolyte phase $L = 10^{-3}$ cm $D = 10^{-5}$ cm^2 s^{-1}	SEI layer $L \sim 10^{-5}$ mm $D = 10^{-5}$ cm^2 s^{-1}	Carbon phase $L =$ part. radius $D = 10^{-9}$ cm^2 s^{-1}
6	0.002	fast	0.025
15	0.002	fast	0.16
44	0.002	fast	1.3

to be 5 mV. This is negligible compared to the total overpotential.

Lithium transport in the electrolyte phase or the SEI does not appear to be the rate-determining step at the rates used in this study. The small characteristic diffusion times associated with Li transport in these two phases does not account for the overpotential that is experimentally observed during discharge/ charge. As the results show in Table 2, Li diffusion in the large graphite particles (SFG44) is expected to be an important factor that limits the high rate performance. This is consistent with the experimental results which showed that the effect of rate on reversible capacity was more pronounced in the graphite with 44 μm particles. The capacity of SFG44 graphite obtained at fast rates ($C/2$) was only 25% of those obtained under equilibrium conditions ($C/24$). This is partially attributable to bulk (solid) diffusion as suggested by the long diffusion times.

3.3. Enhanced capacities with a modified rate programme

Since lithium intercalates into graphite at potentials (< 150 mV vs Li$^+$/Li) close to that for lithium deposition (i.e., cutoff voltage), precautions must be taken to prevent lithium plating. One way to reduce the polarization and to facilitate lithium intercalation is to hold the electrode at a potential close to that of lithium deposition. A modified cycling programme (procedure (ii) in Section 2) containing an additional constant voltage step at 0.005 V was used. This procedure provided maximum capacities for a wide range of carbonaceous materials in our previous studies [3, 18]. It is similar to the potential ending charging method (PECM) used by Zhang [4]. This type of cycling was found to be advantageous for the electrode performance at fast rates. Figure 4 shows a comparison of the potential responses using the two rate programmes at the C rate which illustrates the effect of the constant-potential hold at 0.005 V. An improvement in both the electrode capacity and average discharge voltage can be seen from the voltage curves (bold, dashed line) for SFG6 electrodes that was cycled according to the modified rate programme. At the C rate, the electrode polarized rapidly to the lower potential limit in only 0.1 h. A 2 h hold at 0.005 V allowed it to be fully intercalated. The deintercalation capacity of this electrode, when charged at a

C rate, reached 360 mAh g^{-1}. This is a significant improvement over the capacity of 70 mAh g^{-1} obtained when a discharge procedure without the constant voltage hold step (procedure (i), simplified rate programme) was employed. The constant-potential hold at 5 mV permitted time for additional intercalation of lithium which was completely deinter-calated at the C rate (see Fig. 4). The average charge potential plateau in this case is about 0.5 V, a significant improvement over that obtained using the simple rate programme. It is of interest to note that a large fraction of the overpotential (i.e., 0.38 V) is associated with IR loss. The coulombic efficiencies in these experiments approached 100% after four cycles, suggesting that lithium intercalation/deintercalation occurs reversibly.

The potential profile for lithium deintercalation which results from the use of the modified rate programme was also investigated to verify the electrochemical characteristics of the lithiated graphite particles. Figure 4 includes a charge (solid) profile at $C/24$ rate after the graphite was intercalated rapidly at a C rate followed by a 2 h hold at 0.005 V. Plateaus indicative of staging effects are evident suggesting that the normal lithium storage mechanism (intercalation) takes place in the bulk graphite structure. Furthermore, to ensure the absence of lithium plating during these high-rate experiments, identical electrodes were separatedly discharged to lower potentials that would
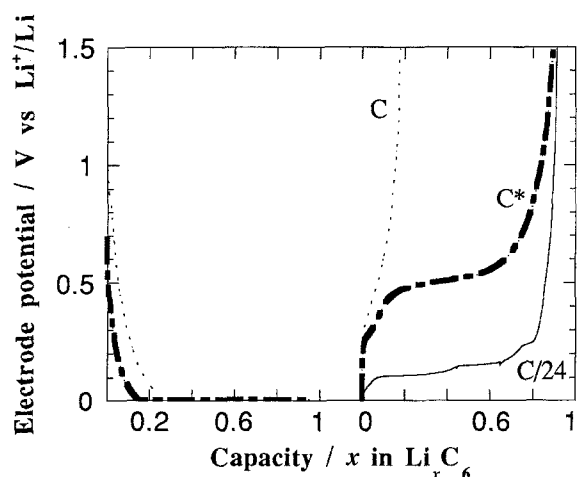

Fig. 4. Voltage curves (first-cycle) for SFG6 electrodes at (a) C rate (dashed line); (b) modified C rate programme (C^*) including a 2 h constant potential hold at 0.005 V (bold dashed line); (c) $C/24$ rate (solid line).

correspond to lithium plating. Deposition of lithium metal was found to occur at −0.050 V vs Li$^+$/Li under these conditions. Cyclic voltammetric experiments [19] with SFG6 electrode at slow scan rates (i.e., 0.012 mV s^{-1}) showed a similar potential at which lithium plating occurred.

The effect of particle size on the charge (deintercalation) rate and lithium storage capacities of fully intercalated electrodes was investigated further. In these experiments, the electrodes were intercalated at different C rates to 0.005 V followed by a constant potential hold at this potential for 2 h. The effect of deintercalation rate on capacities of SFG6 and SFG44 electrodes is shown in Fig. 5. Under the same test conditions, it appears that lithium is completely deintercalated from SFG6 graphite at rates C–C/24, but the large graphite particles (SFG44) exhibit only partial deintercalation at high rates. Because of the slow transport of lithium in the bulk graphite structure, the time is insufficient for the lithium ions to completely intercalate the larger particles, subsequently affecting its deintercalation capacities. The results from both the simple and modified rate studies suggest that the reversible capacity depends strongly on the intercalation rate (e.g., procedure (i)). However, this value is much less dependent on the deintercalation rate if the electrode was fully lithiated. These results are consistent with those reported by Zhang [4] for various types of carbon materials. This has important practical implications as it offers additional means for a quick recharge (intercalation) to provide electrodes that have high-rate capability. In order for the inherently slower intercalation process to keep pace, the discharge programme used above (procedure (ii)) is recommended. This method allowed nearly complete recharging to occur in a significantly shorter period of time.

The graphite materials used in this study have a good cycle life under the cycling procedures involving the constant voltage hold. The capacities of SFG6 graphites (at a modified C/8 rate programme) were nearly unchanged (Li$_{0.95}$C$_6$) with less than a 10% reduction in performance over 200 cycles.

3.4. Effect of rate and particle size on the irreversible capacity loss

The irreversible capacity loss, which is the difference between the first cycle discharge/charge capacities, appears to vary somewhat with the cycling procedure. The relatively smaller capacity loss at high rates suggests that SEI formation may not be completed under such conditions in the first cycle. For the purpose of this discussion, the irreversible capacity loss was determined from the sum of the differences between discharge and charge capacities for the first four cycles. This is plotted as a function of rate for SFG6 graphite in Fig. 6. The irreversible capacity loss associated with the formation of the passivated layer seems to level out at about 68 mAh g^{-1} for lower rates. We normally observed these values at a C/24 rate [3, 18].

Fong et al. [20] have demonstrated that the capacity loss associated with the formation of the solid–electrolyte interphase varied linearly with the carbon surface area. We, however, have not been able to observe a clear relationship between the reported BET surface areas and the capacity losses for the various particles at a given rate (ca. C/24, Table 1) .

4. Summary

The lithium intercalation process is inherently slower than the deintercalation process. This is understandable because the diffusion rate of Li ion is a function of the x value (Li$_x$C$_6$). Experimental measurements [5, 15] showed that the diffusion rate decreases as x increases. Consequently, the Li diffusion rate is lowest when the graphite is fully lithiated, and the rate of deintercalation is slow. On the other hand, the intercalation rate is high initially and becomes more transport limited as intercalation proceeds. This characteristic change in diffusion rate appears to affect the capacity of graphite electrodes at various discharge/charge rate, especially when the discharge rate is not sufficiently slow to ensure complete intercalation.
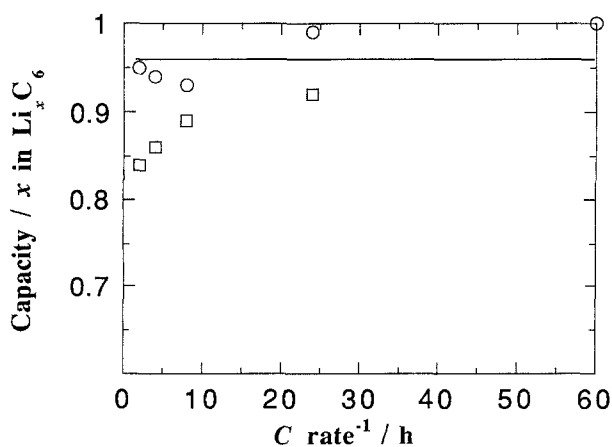

Fig. 5. Effect of the modified rate on SFG6 and SFG44 capacities. Electrodes discharged at indicated rate with a 2 h hold at 0.005 V before charge as in procedure (ii) Section 2. Key: (O) SFG6; (□) SFG44.
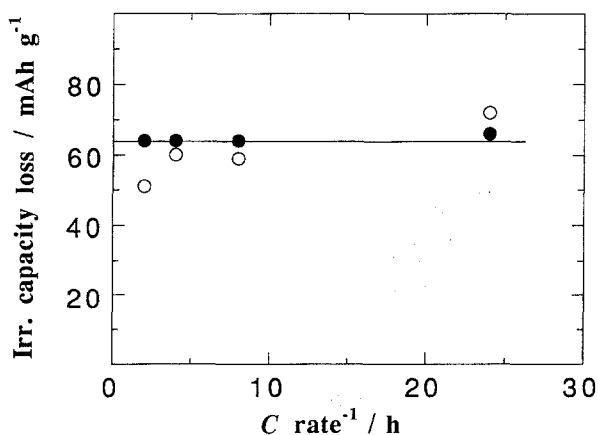

Fig. 6. Plot of irreversible capacities as a function of various rate programmes. The capacity loss was the difference between discharge and charge capacities for the first four cycles for experiments with the modified rate programme (see text). Key: (O) C/n; (●) $C/n + 2$ h at 5 mV.

Deintercalation capacities of fully lithiated graphite with average particle size in the range of 6–44 μm are nearly independent of rate in the range of $C/2$–$C/60$. The ohmic polarization was observed to be an important factor.

Acknowledgement

References

[1] D. Aurbach and Y. Ein-Eli, *J. Electrochem. Soc.* **142** (1995) 1746 .

[2] J. R. Dahn, Simon Fraser University, Burnaby, British Columbia (personal communication).

[3] T. Tran, J. Feikert, X. Song and K. Kinoshita, *J. Electrochem. Soc.* **142** (1995) 3297.

[4] Z. Zhang, *in* 'Rechargeable Lithium and Lithium-Ion Batteries' (edited by S. Megahed, B. Barnett and L. Xie), The Electrochemical Society, Proceedings, vol. 94–28 (1995) p. 165.

[5] N. Takami, A. Satoh, M. Hara and T. Ohsaki, *J. Electrochem. Soc.* **142** (1995) 2564 .

[6] J. M. Tarascon and D. G. Guyomard, Extended Abstracts, volume 93-1, Spring Meeting of the Electrochemical Society, Honolulu, HI, 16–21 May (1993) p. 102.

[7] E Peled, D. Bar-Tow, A. Melman, E. Gerenrot and Y. Lavi,

[8] K. Zaghib, K. Tatsumi, H. Abe, T. Ohsaki, Y. Sawada and S. Higuchi, *in* 'Rechargeable Lithium and Lithium-Ion Batteries', (edited by S. Megahed, B. Barnett and L. Xie), The Electrochemical Society, Proceedings, vol. 94–28 (1995) p. 121.

[9] J. Dahn, A, Sleigh, H. Shi, B. Way, W. Weydanz, J. Reimers, Q. Zhong and U. von Sacken *in* 'Lithium Batteries New Materials, Developments and Perspectives' (edited by G. Pistoia), Elsevier, Amsterdam, The Netherlands (1994) p. 1.

[10] Z. X. Shu, R. S. McMillan and J. J. Murray, *J. Electrochem. Soc.* **140** (1993) 922.

[11] A. J. Bard and L. R. Faulkner, 'Electrochemical Methods-Fundamentals and Applications', J. Wiley & Sons, New York (1980).

[12] K. Zaghib, Hydro-Quebec, Quebec, Canada (personal communication); F. Uribe, Los Alamos National Laboratory, New Mexico (personal communication).

[13] E. Peled, D. Golodnitsky, G. Ardel, C. Menachem, D. Bar Tow and V. Eshkenazy, Materials Research Society Spring Meeting, San Francisco, CA, 17–21 Apr. (1995), abstract W4.1.

[14] N. Takami, A. Satoh, M. Hara and T. Ohsaki, *J. Electrochem. Soc.* **142** (1995) 371.

[15] A. Satoh, N. Takami, M. Hara, and T. Ohsaki, 187th Meeting of the Electrochemical Society, Reno, NV, 21–26 May (1995), abstract 28.

[16] T. Risch and J. Newman, *J. Electrochem. Soc.* **131** (1984) 2551.

[17] J. T. Dudley, D. Wilkinson, G. Thomas, R. LeVae, S. Woo, H. Blom, C. Horvath, M. Juzkow, B. Denis, P. Juric, P. Aghakian and J. Dahn, *J. Power Sources* **35** (1991) 59.

[18] T. D. Tran, J. H. Feikert, S. Mayer, X. Song and K. Kinoshita, *in* 'Rechargeable Lithium and Lithium-Ion Batteries' (edited by S. Megahed, B. M. Barnett and L. Xie), The Electrochemical Society, Proceedings, vol. 94–28 (1995) p. 110.

[19] T. D. Tran and K. Kinoshita, *J. Electroanal. Chem.* **386** (1995) 221.

[20] R. Fong, U. von Sacken and J. R. Dahn, *J. Electrochem. Soc.* **137** (1990) 2009 .